Journal of Intelligent Mechanics and Automation (ISSN Online: 2771-9960)
April 2022 Vol.1, No.1, pp. 21-31
DOI: https://doi.org/10.55571/jima.2022.04023

4D Publishing Group

Influence of Thermal Boundary conditions on Natural Convection Heat Transfer in a Wavy Walled Square Cavity with Adiabatic Block

Shantanu Dutta
Department of Mechanical Engineering, Elitte College of Engineering, Kolkata, India
*Corresponding author's e-mail: shantanudut@gmail.com

Abstract. The aim of the present study is to analyze heat transfer characteristics for natural convection flows in a square enclosure with wavy right wall filled with air(Pr=0.71) having uniform heating on bottom wall and adjacent cold walls with a adiabatic square block inside. This geometry and the following results can be used for analysis in heat management of building architecture, solar collection devices, having walls with surface roughness. The design/methodology/approach of these numerical solutions is the finite element analysis by a commercial software COMSOL Multiphysics version 5.6. The choice of consideration of sinusoidal heating gives a better analysis of heat transfer analysis in this square geometry with wavy wall and with adiabatic block inside has not been investigated by numerical or experimental basis before and therefore, it is this motivation that results in this numerical investigation.

Keywords. Natural convection; Finite element method; Nusselt number: Heat transfer

1. Introduction

Natural convection powered by buoyancy inside a closed cavity is a topic of interest and has been investigated numerically and computationally considering different designs of cavities and enclosed conduits like rhombic [1-4], quadrantal [5-9] rectotrapezoidal [10] and square enclosue [11] and complex enclosures [12-13] considering different boundary situations, enclosure fluid systems and other influencing parameters. While considering the heat transfer inside a closed conduit with a solid insulated rectangular or cylindrical object has several utilities and application in building and architecture construction powered by natural cooling. In such design structure there is a presence of stagnant core of the fluid which doesn't play a lead role while dealing with the convection heat transfer astride the vertical side wall of the cavities [14]. Merrikh and Mohamad [15] in their research article dealt with natural convection in a differentially heated enclosure considering the presence of solid bodies and put forward their conclusions stating that heat transfer might be augmented in presence of a solid body which has a lesser thermal conductivity than that of the fluid participating in heat transfer process and present in the enclosure. Das and Reddy [16] carried out a finite volume

Journal of Intelligent Mechanics and Automation (ISSN Online: 2771-9960)
April 2022 Vol.1, No.1, pp. 21-31
DOI: https://doi.org/10.55571/jima.2022.04023

numerical analysis of natural convection heat transfer in a square cavity considering a block of square dimension and centered (the ratio of solid block to fluid thermal conductivities being taken to be 0.2 and 5.0) and is positioned at center and is also given sufficient inclination at various angles considering the range of 15° to 90° for $Ra = 10^3$–10^6. Another article by Bhave et al. [17] had also reported a natural convection lateral heating study with several numerical deductions and experimentation regarding choosing an best possible adiabatic block dimensions located interior the square enclosure and reported several estimation regarding augmentation of heat transfer considering those block positioning. Merrikh and Lage [18] reported a study on natural convection heat transfer considering a in a square enclosure considering the B.Cs as follow: Vertical walls are subjected to two different temperatures and the horizontal wall being at insulated conditions and with and without a conductive solid block in the center considering the range of $Ra=10^5$ -10^6. In another research article the same authors [19] investigated for an differentially heated enclosure heated and which had a presence of solid square blocks being equally spaced, and also conducting by utilizing continuum model. There were some more interesting work on natural convection and entropy generation involving double isothermal/ insulated square object by Mahapatra et al.[20] and fixed and disconnected solid blocks by Silvio et al.[21]. In another article Datta et al.[22] carried out a porous enclosure natural convection study involving adiabatic blocks comprising of different sizes for the *Da*-*Ra* range of 1–10,000 and with *D*a in the range of $10^{-2} \leq Da \leq 10^{-6}$.

1.1. Problem Description

From the literature analysis it is seen that there has been no study in a wavy walled enclosure considering a solid body with non-uniform heating. Accordingly, the square enclosure being considered is filled with air inside shown in Fig.1 The bottom wall is the hot-wall with non uniform heating and all the remaining wall are subjected to cold temperature, and there is a adiabatic block inside the enclosure of size 0.25L where L is the size of the square enclosure Considering the effect of gravity which is acting in the downward direction(Boussinesq approximation), natural convection heat transfer process is studied numerically inside the complicated enclosure.

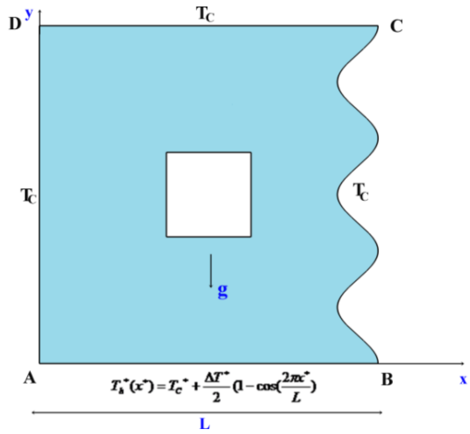

Figure 1. Schematic diagram of the physical model.

1.2. Boundary Conditions

The mathematical equation pertaining to the square enclosure right corrugated wall is:

$$y = \frac{a_n}{L} sin(\phi - \frac{\pi}{2}) sin(\frac{n\pi x}{L}) \tag{1}$$

In the above equation, The dimensionless wave amplitude ($a = a_n/L$) (dimensionless) is kept fixed at= 0.05 For the enclosure of Figure 1, the boundary conditions as discussed earlier and no slip

Journal of Intelligent Mechanics and Automation (ISSN Online: 2771-9960)
April 2022 Vol.1, No.1, pp. 21-31
DOI: https://doi.org/10.55571/jima.2022.04023

velocity flow condition is imposed on all walls. The incompressible fluid being present inside this cavity is newtonian and the flow being also considered as in the laminar range and is steady. The cavity is heated non-uniformly from bottom wall AB, while all the other walls are cooled to a constant temperature. We can express the dimensional form of the non uniform temperature distribution on the bottom heated wall and is adopted from Sarris et al.[23]

$$T_h^*(x^*) = T_C^* + \frac{\Delta T^*}{2}(1-\cos(\frac{2\pi x^*}{L})) \tag{2}$$

where ΔT^* pertains to the temperature difference between the maximum and minimum temperatures of the heated wall, T_c^* pertains to temperatures confined to the cold wall, and L is the length of the enclosure. The dimensionless form of (Eq. (2)) can be re-written by utilizing scale parameters and is adopted from Dalal and Das and Bhardwaj et al. [12-13] and as follow:

$$\theta_w(x) = \frac{1}{2}(1-cos(2\pi x), \theta_{For all other walls} = 0 \tag{3}$$

$$\text{Also, } U = V = 0 \text{ (along AB, BC, CD, DA)} \tag{4}$$

1.3. Governing Equations

We now present the continuity, momentum, and energy equations (Navier stokes 2d) in the laminar thermal flow region of an incompressible newtonian now in this section. There were some other important assumptions being made while representing the equations: (i) absence of viscous dissipation, (ii) the cavity wall being considered as impermeable, (iii) the gravity being active only in vertical (negative y)-direction, (iv) fluid properties being in a state of constant and the fluid density variations are neglected except in the buoyancy term (the Boussinesq approximation) and (v) radiation heat exchange being insignificant because of very small temperature difference.

$$\frac{\partial u^{\otimes}}{\partial x} + \frac{\partial v^{\otimes}}{\partial y} = 0 \tag{5}$$

$$u\frac{\partial u^{\otimes}}{\partial x} + v\frac{\partial u^{\otimes}}{\partial y} = -\frac{1}{\rho}\frac{\partial p}{\partial x} + \nu(\frac{\partial^2 u^{\otimes}}{\partial x^2} + \frac{\partial^2 u^{\otimes}}{\partial y^2}) \tag{6}$$

$$u\frac{\partial v^{\otimes}}{\partial x} + v\frac{\partial v^{\otimes}}{\partial y} = -\frac{1}{\rho}\frac{\partial p}{\partial y} + \nu(\frac{\partial^2 v^{\otimes}}{\partial x^2} + \frac{\partial^2 v^{\otimes}}{\partial y^2}) + g\beta(T - T_c) \tag{7}$$

$$u\frac{\partial T^{\otimes}}{\partial x} + v\frac{\partial T^{\otimes}}{\partial y} = \alpha(\frac{\partial^2 T^{\otimes}}{\partial x^2} + \frac{\partial^2 T^{\otimes}}{\partial y^2}) \tag{8}$$

Now we represent the equations in non-dimensional form.

Journal of Intelligent Mechanics and Automation (ISSN Online: 2771-9960)
April 2022 Vol.1, No.1, pp. 21-31
DOI: https://doi.org/10.55571/jima.2022.04023

$$\left.\begin{array}{l} X=\frac{x}{L};Y=\frac{y}{L},U^{\otimes}=\frac{u^{\otimes}L}{\alpha},V^{\otimes}=\frac{v^{\otimes}L}{\alpha}, \\ \theta^{\otimes}=\frac{T^{\otimes}-T_c}{T_h-T_c},p=\frac{pL^2}{\rho\alpha^2},\Pr=\frac{\nu}{\alpha}, \\ Ra=\frac{g\beta(T_h-T_c)L^3\Pr}{\nu^2}/=\frac{c_p\rho^2 g\beta TL^3}{\mu k} \end{array}\right\} \tag{9}$$

$$\frac{\partial U^{\otimes}}{\partial X}+\frac{\partial V^{\otimes}}{\partial Y}=0, \tag{10}$$

$$U\frac{\partial U^{\otimes}}{\partial X}+V\frac{\partial V^{\otimes}}{\partial Y}=-\frac{\partial P}{\partial X}+\Pr\left(\frac{\partial^2 U^{\otimes}}{\partial X^2}+\frac{\partial^2 U^{\otimes}}{\partial Y^2}\right) \tag{11}$$

$$U\frac{\partial V^{\otimes}}{\partial X}+V\frac{\partial V^{\otimes}}{\partial Y}=-\frac{\partial P}{\partial Y}+\Pr\left(\frac{\partial^2 V^{\otimes}}{\partial X^2}+\frac{\partial^2 V^{\otimes}}{\partial Y^2}\right)+Ra*\Pr*\theta \tag{12}$$

$$U\frac{\partial \theta^{\otimes}}{\partial X}+V\frac{\partial \theta^{\otimes}}{\partial Y}=\frac{\partial^2 \theta^{\otimes}}{\partial X^2}+\frac{\partial^2 \theta^{\otimes}}{\partial Y^2} \tag{13}$$

1.4. Nusselt Number

The heat transfer coefficient can be expressed in terms of local Nusselt number (Nu) and as follow:

$Nu=-\frac{\partial\theta}{\partial n}$ where n denotes the normal direction on a plane.

$$Nu_b=-\frac{\partial\theta}{\partial Y} \tag{14}$$

The average Nusselt number on the different walls are given by the expression:

$$\overline{Nu_b}=\frac{\int_0^1 Nu_b dX}{X_0^1}=\int_0^1 Nu_b\ dX,\quad \overline{Nu_l}=\int_0^1 Nu_l dS_1,\quad \overline{Nu_r}=\int_0^1 Nu_r dS_2 \tag{15}$$

2. Numerical Solution Methodology and Model Validation

The governing transport equations after converting into non –dimensional form (Eqs.10-13) and (Eqs 2-3) as are solved by commercial software COMSOL (finite element) Multiphysics. The galerkin weighted method is utilized for transforming the governing equations into a system of integral equation and can be look into for detailed description in Zienkiewicz et al. [24]. The convergence criterion is controlled in a manner that $\left|\phi^{n+1}-\phi^{n}\right|/\phi^{n}\leq 10^{-6}$, where ϕ_t represents any transport variable. The results obtained from the present numerical scheme have been validated against the results of Bhave et al.[12] for a square cavity filled with a air (Pr=0.71) for the isotherms and streamlines when the left wall is uniformly heated and the right vertical wall is cold. Another validation of present Nu results with conducting block was carried out by comparing the published results of average Nu of House [1] and Merrick and Lage[18]. Its found that results are very similar.

Table 1 : Comparison of Average Nu considering (block) thermal conductivity and Φ (solidity).

Journal of Intelligent Mechanics and Automation (ISSN Online: 2771-9960)
April 2022 Vol.1, No.1, pp. 21-31
DOI: https://doi.org/10.55571/jima.2022.04023

Ra	Φ	K	Present	House [1]	Merrick and Lage[18]
10^6	0.5	0.2	4.569	4.624	4.605
10^6	0.5	5.0	4.386	4.324	4.28
10^7	0.9	0.2	2.387	2.402	2.352

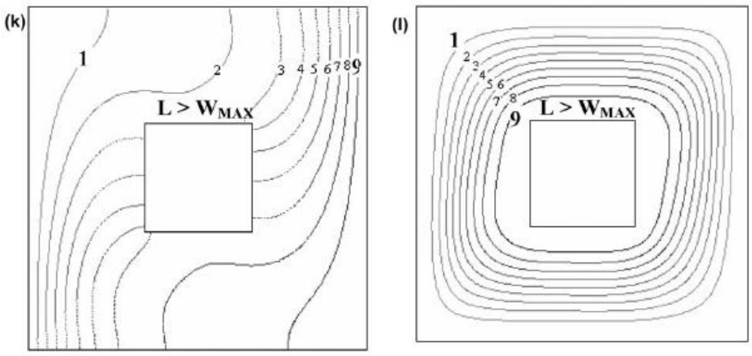

(a)

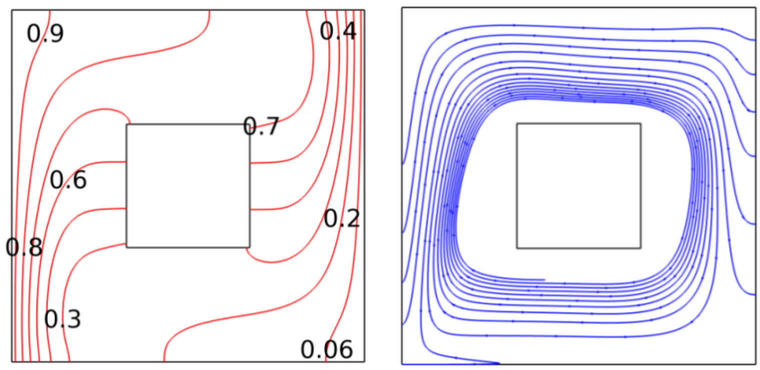

(b)

Figure 2: Validation results of Streamline isotherm comparison from (a) Published literature[17]; (b) Present results.

Table 2: Comparisonof ($\overline{Nu}$) on the bottom wall for different grid systems with [uniform heating of bottom wall] for same BC , square Enclosure.

Ra	No of elements			Relative Error % (max-min)/max
	5314	11300	28010	
10^3	1.4248	1.4273	1.4288	0.105
10^4	1.4999	1.5023	1.5039	0.106
10^5	2.9634	2.9601	2.9611	0.034
10^6	5.7295	5.7591	5.9245	2.79

A grid independence test has also been carried out to establish that the results are independent of the grid used for numerical simulation. The values of averaged Nusselt number ($\overline{Nu}$)on the uniformly heated bottom wall for different grid systems are presented in Table 1. It has been proposed to use 11300 elements for numerical simulation, because of the fact that when the number of elements increase from 11300 to 28010, the maximum relative error recorded is 2.79%.

Journal of Intelligent Mechanics and Automation (ISSN Online: 2771-9960)
April 2022 Vol.1, No.1, pp. 21-31
DOI: https://doi.org/10.55571/jima.2022.04023

3. Results and Discussions

3.1. Analysis of Stream lines and Isotherm

We now present the heat transfer and fluid flow characteristics in the following square geometry considering non-uniformly heated bottom wall. The flow distributions are presented via isotherms and streamlines. The Prandtl number of fluid is chosen to be 0.71. By, examining Figure 3 left and right panel plot which shows streamlines and isotherms obtained numerically for Ra = 10^3-10^6 we observe that streamlines(right panel plot) are forming straight lines emanating from the non uniform bottom wall with very weak streamline strength of ψ_{max} =0.181. Increasing the value of Rayleigh number increase the streamline strength to ψ_{max}=1.93 and the cumulative nature of streamline is similar to Ra=10^3. With further increase of streamline strength to Ra=10^5 and Ra=10^6 changes the complete orientation of streamline . A single cell of elliptical shape is seen to rotate along the insulated block and the value of positive streamline ψ_{max} =11.54 is observed. The negative value of streamline strength moving in clockwise direction has a strength of ψ_{min} =-23.52 For further increase of Rayleigh number to Ra=10^6 the primary roll breaks up into several secondary rolls and due to presence of strong thermal boundary layer the maximum and minimum value of stream line contour are observed to 100 (counter clockwise orientation) and 67 for clockwise orientation (as per sign convection). So magnitude of stream line contour shows the highest value in case of Ra=10^6. The left panel plots of Figure 3 show isotherms and they demonstrate several twisting and has a tendency of shifting towards the left cold wall and this tendency is more at higher Ra=10^5 and 10^6 due to increase of natural convection effects with increase of Rayleigh number. At lower values of Ra=10^3 and 10^4 the isotherm patterns demonstrate conduction like effect with no twisting of isotherm and they only partially fill up of the enclosure.

3.2. Local Nusselt Number:

Local Nusselt numbers for left, top and right cold wall and bottom heated wall for different sets of Ra for presented for the case of non-uniform heating case. It's clear from these figures, that local Nusselt number for bottom wall. Figure 4(a) depict an increasing decreasing trend all along the length of enclosure, for all values of Ra number and its maximum value is around 12(for dimensionless distance X=0.3) for Ra=10^6 . Local Nu for the left , right and the top wall (Figure 4 c, d and b) are all negative values reiterating the fact that heat is transferred from the fluid to the wall in all these cases. The right wall has a very interesting local Nu profile as because of the imposed temperature profile in the right wall. The minimum value of Nu_r=7 for Ra=10^6 (at X=0.95)for right vertical cold wall.

3.3. Average Nusselt number

Average Nusselt number has been depicted in Table 2 and 3. Table 2 shows the values of for ($\overline{Nu}$) bottom wall, top wall left wall, right wall for different values of Rayleigh number with block whereas Table 3 depicts the ($\overline{Nu}$)for bottom wall for different values of Rayleigh number without block. It is observed that surprisingly the $\overline{Nu}$ for bottom wall without block is not distinctly different for the case with block. The values progressively increase with increase of Ra and all values of top wall left wall and right wall are negative and heat is transferred from the fluid to the wall in all these cases.

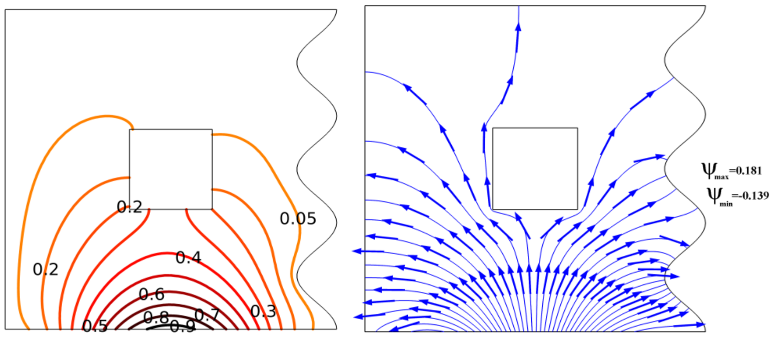

(a)

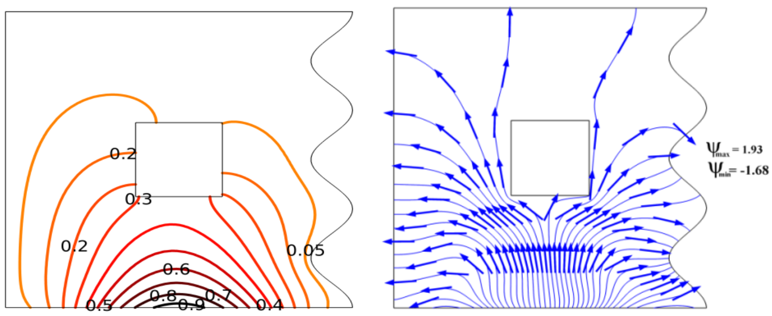

(b)

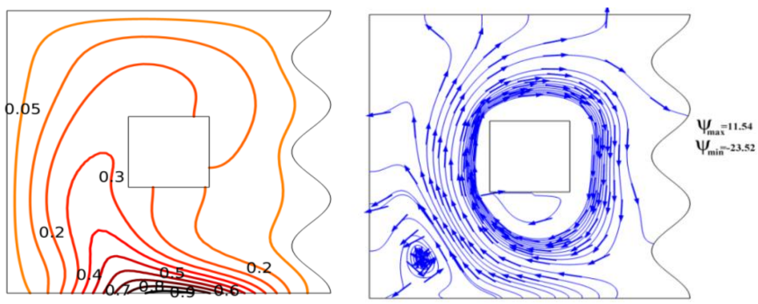

(c)

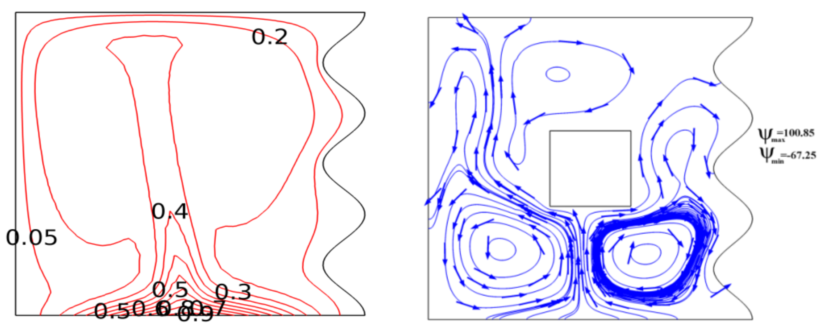

(d)

Figure 3. Isotherms (left); Streamlines (right) (a) Ra=10^3 (b) Ra=10^4 (c) Ra=10^5 and (d) Ra=10^6.

Journal of Intelligent Mechanics and Automation (ISSN Online: 2771-9960)
April 2022 Vol.1, No.1, pp. 21-31
DOI: https://doi.org/10.55571/jima.2022.04023

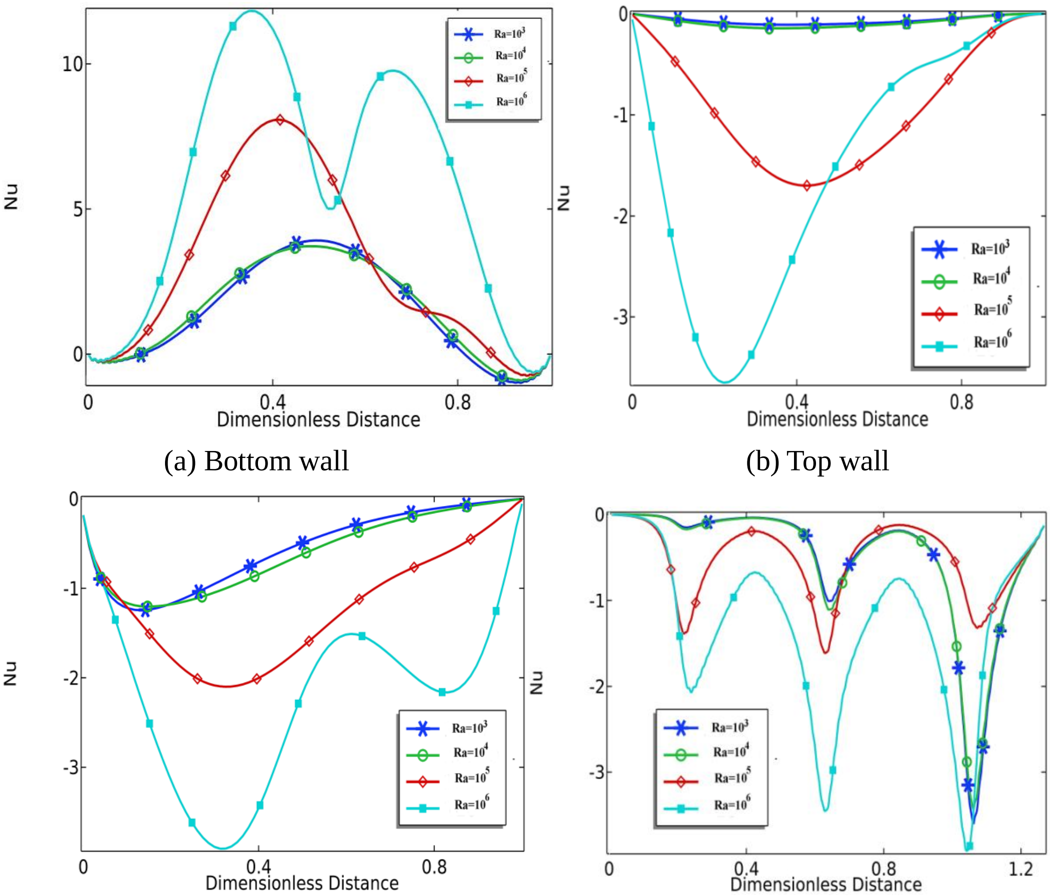

(a) Bottom wall

(b) Top wall

(c) Left wall

(d) Right wall

Figure 4. Local Nusselt numbers for different wall positions.

Table 2. ($\overline{Nu}$) for bottom wall, top wall left wall, right wall for different range of *Ra* with block.

Ra	$\overline{Nu}_b$	$\overline{Nu}_r$	$\overline{Nu}_l$	$\overline{Nu}_T$
10^3	1.4273	0.65728	-0.55458	-0.065806
10^4	1.5023	-0.65946	-0.60720	-0.084555
10^5	2.9601	-0.66092	-1.2247	-0.91692
10^6	5.7591	-1.6358	-2.2124	-1.4997

Table 3. ($\overline{Nu}$)for bottom wall considering different range of *Ra* without block.

Ra	$\overline{Nu}_b$
10^3	1.4964
10^4	1.6636
10^5	3.3767
10^6	5.7332

4. Conclusions

The study of buoyancy assisted heat transfer in a square enclosure filled with air has been studied numerically in a square cavity with adiabatic block. The effect of Rayleigh number on the heat transfer is examined.. The results of the numerical analysis lead to the following conclusions:

1) The nature of isotherms have a pattern of shifting towards the left cold wall and this tendency is more at higher $Ra=10^5$ and 10^6 due to increase of natural convection effects with increase of Rayleigh number.

2) The maximum value of magnitude of ψ is 100(+ve, anti-clockwise orientation) for non-uniform heating for $Ra=10^6$, and specially at higher $Ra\geq10^5$ heat transfer occurs due to convection. At lower values of *Ra* heat transfer is primarily manifested in weak circulation strength and it this is due to effect of conduction at $Ra=10^3$.

3) Local Nusselt number shows an increase decrease trend and maximum value of local Nu is around 12 for $Ra=10^6$.

Acknowledgements
The author has not received any fund for carrying out this research work. The authors acknowledge the support of IIT Khargapur CFD lab, Mechanical engineering department.

Conflicts of Interest
The author indicate that there is no conflict of interest.

Appendix

NOMENCLATURE

c_p Specific heat ($Jkg^{-1}K^{-1}$)
g Acceleration due to gravity (ms^{-2})
H Enclosure height (m)
h Heat transfer coefficient (Wm^2K^{-1})
k Thermal conductivity ($W\ m^{-1}, K^{-1}$)
L Enclosure length (m)
$\overline{Nu}$ Average Nusselt Number
Nu Nusselt number (dimensionless)
P Non-dimensional pressure
p Pressure (Nm^2)
Pr Prandtl number (dimensionless)
Ra Rayleigh number (dimensionless)
T Temperature (K)
U ,V Non-dimensional velocity component in the X and Y direction
u, v Velocity component in the x and y direction (ms^{-1})
X, Y Non-dimensional coordinates
x, y Cartesian coordinate system

Greek symbols

α Thermal diffusivity (m^2s^{-1})
β Co-efficient of thermal expansion (K^{-1})
θ Dimensionless temperature
ν Kinematic viscosity (m^2s^{-1})
ρ Density(kgm^{-3})
ψ Stream function (m^2 s)
Ψ Non-dimensional stream

Φ solidarity function (=ψ /α) of the enclosure = Ab/A = L^2.

Subscripts

c Cold wall
h Hot, bottom wall
max Maximum
min Minimum

References

[1] [1]Dutta, S., Goswami, N., Biswas, A.K. and Pati, S., 2019. Numerical investigation of magnetohydrodynamic natural convection heat transfer and entropy generation in a rhombic enclosure filled with Cu-water nanofluid. *International Journal of Heat and Mass Transfer*, *136*, pp.777-798.
[2] [2]Dutta, S., Goswami, N., Pati, S. and Biswas, A.K., 2021. Natural convection heat transfer and entropy generation in a porous rhombic enclosure: influence of non-uniform heating. *Journal of Thermal Analysis and Calorimetry*, *144*(4), pp.1493-1515.
[3] [3]Dutta, S., Biswas, A.K. and Pati, S., 2019. Analysis of natural convection in a rhombic enclosure with undulations of the top wall–a numerical study. *International Journal of Ambient Energy*, pp.1-11.
[4] [4]Dutta, S., Pati, S. and Biswas, A.K., 2020. Thermal transport analysis for natural convection in a porous corrugated rhombic enclosure. *Heat Transfer*, *49*(6), pp.3287-3313.
[5] [5]Dutta, S. and Pati, S., 2022. Magnetohydrodynamic Natural Convection in a Quadrantal Enclosure. *Journal of Thermophysics and Heat Transfer*, pp.1-15.
[6] [6]Dutta, S., Biswas, A.K. and Pati, S., 2018. Natural convection heat transfer and entropy generation inside porous quadrantal enclosure with nonisothermal heating at the bottom wall. *Numerical Heat Transfer, Part A: Applications*, *73*(4), pp.222-240.
[7] [7]Dutta, S., Pati, S. and Baranyi, L., 2021. Numerical analysis of magnetohydrodynamic natural convection in a nanofluid filled quadrantal enclosure. *Case Studies in Thermal Engineering*, *28*, p.101507.
[8] [8]Dutta, S., Biswas, A.K. and Pati, S., 2019. Numerical analysis of natural convection heat transfer and entropy generation in a porous quadrantal cavity. *International Journal of Numerical Methods for Heat & Fluid Flow*.
[9] [9]Dutta, S. and Biswas, A., 2018. Entropy generation due to natural convection with non-uniform heating of porous quadrantal enclosure-a numerical study. *Frontiers in Heat and Mass Transfer (FHMT)*, *10*.
[10] [10]Dutta, S. and Biswas, A.K., 2019. A numerical investigation of natural convection heat transfer of copper-water nanofluids in a rectotrapezoidal enclosure heated uniformly from the bottom wall A numerical investigation of natural convection heat transfer of copper-water nanofluids in a rectotrapezoidal enclosure heated uniformly from the bottom wall. *Math Model Eng Prob*, *6*(1), pp.105-114.
[11] [11]Dutta, S. and Pati, S., 2021. Influence of Thermal Radiation on Natural Convection in a Square Enclosure. In *Techno-Societal 2020* (pp. 513-524). Springer, Cham.
[12] [12]Dalal A. and Das, M. K., (2005),"Laminar Natural Convection in an Inclined Complicated Cavity with Spatially Variable Wall Temperature", International Journal of Heat and Mass Transfer, 48, 3833–3854. **http://dx.doi.org/10.1016/j.ijheatmasstransfer.2004.07.051**.
[13] [13] Bhardwaj, S., Dalal, A. and Pati, S., 2015. Influence of wavy wall and non-uniform heating on natural convection heat transfer and entropy generation inside porous complex enclosure. *Energy*, *79*, pp.467-481.
[14] [14]J.M. House, C. Beckermann, T.F. Smith, Effect of a centered conducting body on natural convection heat transfer in an enclosure,Num. Heat Transfer Part A 18 (1990) 213–225.

Journal of Intelligent Mechanics and Automation (ISSN Online: 2771-9960)
April 2022 Vol.1, No.1, pp. 21-31
DOI: https://doi.org/10.55571/jima.2022.04023

[15] [15]A. A. Merrikh and A. A. Mohamad, Blockage Effects in Natural Convection in Differentially Heated Enclosures, Enhanced Heat Transfer, vol. 8, pp. 55–72, 2000.

[16] [16]M. K. Das and K. S. K. Reddy, Conjugate Natural Convection Heat Transfer in an Inclined Square Cavity Containing a Conducting Block, Int. J. Heat Mass Transfer,vol. 49, pp. 4987–5000, 2006.

[17] [17]Bhave, P., Narasimhan, A. and Rees, D.A.S., 2006. Natural convection heat transfer enhancement using adiabatic block: optimal block size and Prandtl number effect. *International Journal of Heat and Mass Transfer*, *49*(21-22), pp.3807-3818.

[18] [18] Merrikh AA, Lage JL. (2004)Effect of distributing a fixed amount of solid constituent inside a porous medium enclosure on the heat transfer process. Proceedings of International Conference on Applications of Porous Media(ICAPM):51–58, Évora, Portugal.

[19] [19]Merrikh, A.A. and Lage, J.L., 2005. Natural convection in an enclosure with disconnected and conducting solid blocks. *International Journal of Heat and Mass Transfer*, *48*(7), pp.1361-1372.

[20] [20]Mahapatra, P.S., De, S., Ghosh, K., Manna, N.K. and Mukhopadhyay, A., 2013. Heat transfer enhancement and entropy generation in a square enclosure in the presence of adiabatic and isothermal blocks. *Numerical Heat Transfer, Part A: Applications*, *64*(7), pp.577-596.

[21] [21]Junqueira, S.L., De Lai, F.C., Franco, A.T. and Lage, J.L., 2013. Numerical investigation of natural convection in heterogeneous rectangular enclosures. *Heat transfer engineering*, *34*(5-6), pp.460-469.

[22] [22] Datta, P., Mahapatra, P.S., Ghosh, K., Manna, N.K. and Sen, S., 2016. Heat transfer and entropy generation in a porous square enclosure in presence of an adiabatic block. *Transport in Porous Media*, *111*(2), pp.305-329.

[23] [23] I. E. Sarris, I. Lekakis and N. S. Vlachos, “Natural Convection in a 2D Enclosure with Sinusoidal Upper Wall Temperature,” Numerical Heat Transfer, Part A, Vol. 42, No. 5, 2002, pp. 513-530. doi:10.1080/10407780290059675 .

[24] [24] Zienkiewicz, O.C., Taylor, R.L., Nithiarasu, P. and Zhu, J.Z., 1977. *The finite element method* (Vol. 3). London: McGraw-hill.